LA-UR-12-21918
Approved for public release; distribution is unlimited.

Title: Distinguishing S-plus-minus and S-plus-plus electron pairing symmetries by neutron spin resonances in superconducting Sodium-Iron-Cobalt-Arsenic (transitional temperature = 18 Kelvin)

Author(s):
Das, Tanmoy
Balatsky, Alexander V.
Zhang, Chenglin
Li, Haifeng
Su, Yiki
Nethertom, Tucker
Redding, Caleb
Carr, Scott
Schneidewind, Astrid
Faulhaber, Enrico
Li, Shiliang
Yao, Daoxin
Bruckel, Thomas
Dai, Pengchen
Sobolev, Oleg

Intended for: Nature Communication

Distinguishing $s^{\pm}$ and s^{++} electron pairing symmetries by neutron spin resonance in superconducting $NaFe_{0.935}Co_{0.045}As$

Chenglin Zhang,[1,*] H.-F. Li,[2,3] Yixi Su,[4] Guotai Tan,[5,1] Yu Song,[1] Tucker Netherton,[1] Caleb Redding,[1] Scott V. Carr,[1] Oleg Sobolev,[6] Astrid Schneidewind,[7] Enrico Faulhaber,[8,7] Shiliang Li,[9] Daoxin Yao,[10] Tanmoy Das,[11] A. V. Balatsky,[11] Th. Brückel,[12] and Pengcheng Dai[1,9,†]

[1] *Department of Physics and Astronomy, The University of Tennessee, Knoxville, Tennessee 37996-1200, USA*
[2] *Jülich Centre for Neutron Science JCNS, Forschungszentrum Jülich GmbH, Outstation at Institut Laue-Langevin, Boîte Postale 156, F-38042 Grenoble Cedex 9, France*
[3] *Institut für Kristallographie der RWTH Aachen, 52056 Aachen, Germany*
[4] *Jülich Centre for Neutron Science JCNS-FRM II, Forschungszentrum Jülich GmbH, Outstation at FRM II, Lichtenbergstrasse 1, D-85747 Garching, Germany*
[5] *College of Nuclear Science and Technology, Beijing Normal University, Beijing 100875, China*
[6] *Institut für Physikalische Chemie, Georg-August-Universität Göttingen, Tammannstrasse 6, 37077 Göttingen, Germany*
[7] *Forschungsneutronenquelle Heinz Maier-Leibnitz (FRM-II), TU München, D-85747 Garching, Germany*
[8] *Gemeinsame Forschergruppe HZB - TU Dresden, Helmholtz-Zentrum Berlin für Materialien und Energie, D-14109 Berlin, Germany*
[9] *Beijing National Laboratory for Condensed Matter Physics, Institute of Physics, Chinese Academy of Sciences, Beijing 100190, China*
[10] *State Key Laboratory of Optoelectronic Materials and Technology, Sun Yat-Sen University, Guangzhou 510275, China*
[11] *Theoretical Division, Los Alamos National Laboratory, Los Alamos, NM, 87545, USA*
[12] *Jülich Centre for Neutron Science JCNS and Peter Grünberg Institut PGI, JARA-FIT, Forschungszentrum Jülich GmbH, 52425 Jülich, Germany*

A determination of the superconducting (SC) electron pairing symmetry forms the basis for establishing a microscopic mechansim for superconductivity. For iron pnictide superconductors, the $s^{\pm}$-pairing symmetry theory predicts the presence of a sharp neutron spin resonance at an energy below the sum of hole and electron SC gap energies ($E \leq 2\Delta$). Although the resonances have been observed for various iron pnictide superconductors, they are broad in energy and can also be interpreted as arising from the s^{++}-pairing symmetry with $E \geq 2\Delta$. Here we use inelastic neutron scattering to reveal a sharp resonance at $E = 7$ meV in the SC $NaFe_{0.935}Co_{0.045}As$ ($T_c = 18$ K). By comparing our experiments with calculated spin-excitations spectra within the $s^{\pm}$ and s^{++}-pairing symmetries, we conclude that the resonance in $NaFe_{0.935}Co_{0.045}As$ is consistent with the $s^{\pm}$-pairing symmetry, thus eliminating s^{++}-pairing symmetry as a candidate for superconductivity.

PACS numbers: 74.25.Ha, 74.70.-b, 78.70.Nx

A determination of the superconducting (SC) electron pairing symmetry is an important step to establish a microscopic theory for high-transition temperature (high-T_c) superconductivity [1]. Since the discovery of iron pnictide superconductors [2–4], a peculiar unconventional pairing state, where superconductivity arises from sign-revised quasiparticle excitations between the isotropic hole and electron Fermi pockets near the Γ and M points, respectively, has been proposed [5–7]. A consequence of this so-called $s^{\pm}$-pairing state is that the sign-reversed quasiparticle excitations necessitate a sharp resonance in the spin excitations spectra (termed spin resonance) occurring below the sum of the hole and electron SC gap energies ($E \leq 2\Delta = \Delta_h + \Delta_e$) at the antiferromagnetic (AF) wave vector $\mathbf{Q}$ connecting the two Fermi surfaces [8, 9]. Although the experimental discovery of the resonance by neutron scattering in hole and electron-doped $BaFe_2As_2$ iron pnictide superconductors has been hailed as evidence for the $s^{\pm}$-pairing symmetry [10–20], the mode is broad in energy and may not satisfy $E \leq 2\Delta$ [21–23]. Furthermore, transport and nuclear magnetic resonance (NMR) experiments [24] reveal a lack of strong impurity effect, contrary to the expectation of the $s^{\pm}$-pairing symmetry [25]. Finally, resonant ultrasound spectroscopy on the parent and optimally electron doped $BaFe_2As_2$ indicates a strong AF order-electron-lattice coupling that is not expected within the $s^{\pm}$-pairing theory [26]. Instead, these results may be interpreted as the orbital fluctuation mediated s^{++}-pairing superconductivity, where one expects a broad neutron spin resonance at an energy of $E \geq 2\Delta$ [21, 22].

Here we present inelastic neutron scattering results on single crystals of SC $NaFe_{0.935}Co_{0.045}As$ with $T_c = 18$ K (see Fig. 1). In the normal state, the imaginary part of the dynamic susceptibility, $\chi''(\mathbf{Q}, E)$, at the AF wave vector increases linearly with increasing energy E. Upon entering into the SC state, a spin gap opens below 5.5 meV and a sharp neutron spin resonance appears at $E = 7$ meV with an energy width of $\sim$2 meV. By comparing the neutron scattering results with a random-phase approximation (RPA) spin-susceptibility calculation within the s^{+-} and s^{++}

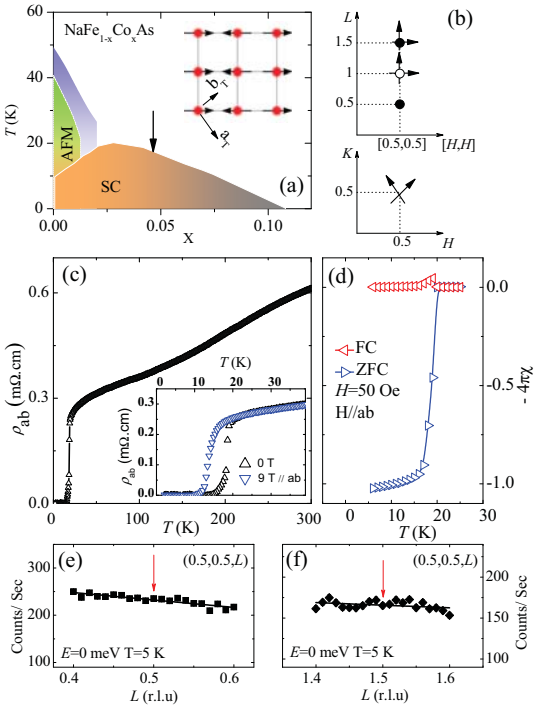

FIG. 1: **Phase diagram, real, reciprocal space, transport, and susceptibility measurements.** (a) The electronic phase diagram of $NaFe_{1-x}Co_xAs$, where the arrow indicates the Co-doping level of our samples. Inset shows the in-plane AF structure of NaFeAs [27]. (b) Reciprocal space probed in the present experiment. The scan directions are shown as arrows. (c) Temperature dependence of the in-plane resistivity ρ_{ab} in $NaFe_{0.935}Co_{0.045}As$. The inset displays the low-T resistivity measured in zero-field and 9 T. (d) The temperature dependence of the bulk susceptibility measured by DC magnetic susceptibility. (e) and (f) Elastic neutron scattering from PUMA along the $[0.5, 0.5, L]$ directions at 5 K. The solid lines are guided to the eyes and the arrows indicate the positions of AFM static ordering.

pairings, we find that our data are consistent with the s^{+-} symmetry, thus ruling out s^{++}-pairing as a candidate for superconductivity.

Results

Sample and experimental Details We carried out inelastic neutron scattering experiments on the thermal (PUMA) and cold (PANDA) triple-axis spectrometers at the FRM-II, TU Müchen, Germany. For the experiments, we coaligned 5 pieces of self-flux grown $NaFe_{1-x}Co_xAs$ single crystals with a total mass of 5.5 g (mosaic about 1.5°). The chemical compositions of the samples are determined as $Na_{1.06}Fe_{0.935}Co_{0.045}As$ by inductively coupled plasma atomic-emission spectroscopy, which we denote as $NaFe_{0.935}Co_{0.045}As$. The wave vector **Q** at (q_x,q_y,q_z) in $Å^{-1}$ is defined as $(H,K,L) = (q_xa/2\pi, q_ya/2\pi, q_zc/2\pi)$ reciprocal lattice unit (r.l.u) using the tetragonal unit cell (space group P4/nmm, $a = 3.921$ Å, $c = 6.911$ Å at 5 K). We used focusing pyrolytic graphite (PG) monochromator and analyzer with fixed final energies of $E_f = 14.7$ meV and $E_f = 5$ meV at PUMA and PANDA, respectively. Both the $[H, H, L]$ and $[H, K, 0]$ scattering zones have been used in the experiments and the scan directions are marked in Fig. 1(b). To characterize the samples, we have carried out resistivity and DC magnetic susceptibility measurements using commercial physical property measurement system and SQUID magnetometer. Based on the early neutron diffraction measurements [27], AF Bragg peaks and low-energy spin excitations are expected to occur around the $(0.5, 0.5, L)$ positions with $L = 0.5, 1.5, \cdots$ [Fig. 1(b)].

Figure 1(c) plots the in-plane resistivity ρ_{ab} measurement at zero field which gives $T_c = 18$ K. The inset shows the magnetic field dependence of ρ_{ab} at 0 and 9-T, indicating a field-induced T_c suppression of ∼2 K. Figure 1(d) shows the magnetic susceptibility measurements on the sample again showing a $T_c = 18$ K. Given the known electronic phase diagrams of $NaFe_{1-x}Co_xAs$ [28, 29], it is clear that our $NaFe_{0.935}Co_{0.045}As$ samples are in the slightly overdoped regime and do not have static AF order coexisting with superconductivity [Figs. 1(a)]. Our elastic neutron diffraction scans through the AF Bragg peak positions are featureless and thus confirm this conclusion [Figs. 1(e) and 1(f)].

Neutron Scattering Results In previous neutron scattering work on electron doped $BaFe_{2-x}Ni_xAs_2$ pnictide

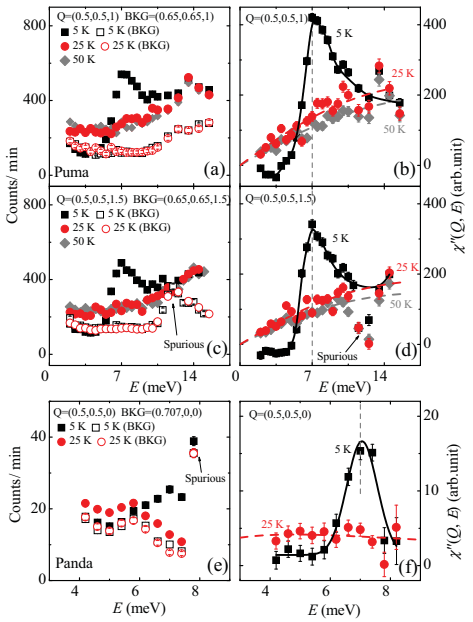

FIG. 2: **Energy scans at the AF wave vector.** (a) and (c) Energy scans at $\mathbf{Q} = (0.5, 0.5, 1)$ and $\mathbf{Q} = (0.5, 0.5, 1.5)$, respectively, at 5, 25, and 50 K on PUMA. The background was taken at $\mathbf{Q} = (0.65, 0.65, 1)$ and $\mathbf{Q} = (0.65, 0.65, 1.5)$, respectively, at 5 and 25 K. (b) and (d) are the corresponding $\chi''(Q, E)$.(e) Energy scans at $\mathbf{Q} = (0.5, 0.5, 0)$ and the background $\mathbf{Q} = (0.707, 0, 0)$ at 5 and 25 K on PANDA. (f) is the corresponding $\chi''(Q, E)$. The solid and dashed lines are guides to the eyes. The vertical dashed lines indicate the resonance energy.

superconductors [14, 17], the neutron spin resonance was found to be dispersive, occurring at slightly different energies for different c-axis wave vector transfers. To see if this is also the case for spin excitations in $NaFe_{0.935}Co_{0.045}As$, we carried out constant-$\mathbf{Q}$ scans at wave vectors $\mathbf{Q} = (0.5, 0.5, 1)$ and $(0.5, 0.5, 1.5)$ below and above T_c on PUMA. While the background scattering (BKG) taken at $\mathbf{Q} = (0.65, 0.65, 1)$ and $(0.65, 0.65, 1.5)$ showed no change below and above T_c [Figs. 2(a) and 2(c)], the scattering at the in-plane AF wave vector revealed dramatic changes across T_c. In the normal state ($T = 25$ K), the scattering above BKG is featureless and increases with increasing energy. Upon entering into the SC state ($T = 5$ K), a spin gap forms below ∼5.5 meV and a sharp resonance appears at $E = 7$ meV [Figs. 2(a) and 2(c)]. The corresponding $\chi''(Q, E)$, obtained by subtracting the BKG and correcting for the Bose population factors using $\chi''(Q, E) = [1 - \exp(-E/k_BT)]S(Q, E)$, are shown in Figs. 2(b) and 2(d). Inspection of Figs. 2(a)-2(d) reveals that the resonance exhibits no c-axis dispersion and has an energy width of ∼3 meV. Figures 2(e) and 2(f) show similar scans on PANDA, which reveal a 6 meV spin gap and a sharp resonance at $E = 7$ meV with an energy width of ∼1.6 meV in the SC state. This is much narrower than the energy widths of the resonances in the hole and electron-doped $BaFe_2As_2$ [10–19].

To confirm the SC spin gap and determine the wave vector dependence of the resonance, we carried out constant-energy scans at $E = 4, 7$, and 15 meV below and above T_c. Figures 3(a-c) and 3(d-f) show $\chi''(Q, E)$ along the $[H, H, 1]$ and $[H, H, 1.5]$ directions, respectively. In the SC state at $T = 5$ K, $\chi''(Q, E)$ is featureless at $E = 4$ meV and thus confirms the presence of a spin gap. For other excitation energies, the scattering profiles can be fitted by Gaussians on linear BKG. By Fourier transforms of the fitted Guassian peaks along the $[H, H, 1]$ direction, we find that the in-plane spin-spin correlation lengths of the resonance are $\xi = 24 \pm 1$ Å at 25 K and $\xi = 30 \pm 1$ Å at 5 K. Along the $[H, H, 1.5]$ direction, $\xi = 32 \pm 3$ Å are unchanged from 25 K to 5 K. Increasing the excitation energy to $E = 15$ meV ($> 2\Delta$), there are no observable differences in scattering intensity and spin correlation lengths ($\xi = 20 \pm 1$ Å) below and above T_c

Figure 4(a) shows the temperature dependence of the scattering at the AF wave vector $\mathbf{Q} = (0.5, 0.5, 1.5)$ for the resonance ($E = 7$ meV) and spin gap ($E = 4$ meV) energies. While the intensity increases dramatically below T_c at the resonance energy, it decreases at $E = 4$ meV signaling the opening of a SC spin gap. To test if spin excitations in $NaFe_{0.935}Co_{0.045}As$ are indeed two-dimensional in reciprocal space like in the case of Co-doped $BaFe_2As_2$ [13], we show in Fig. 4(b) BKG subtracted constant-energy scans along the $[0.5, 0.5, L]$ direction at the resonance energy ($E = 7$ meV) below and above T_c. The monotonic decrease of the scattering with increasing L is consistent with the

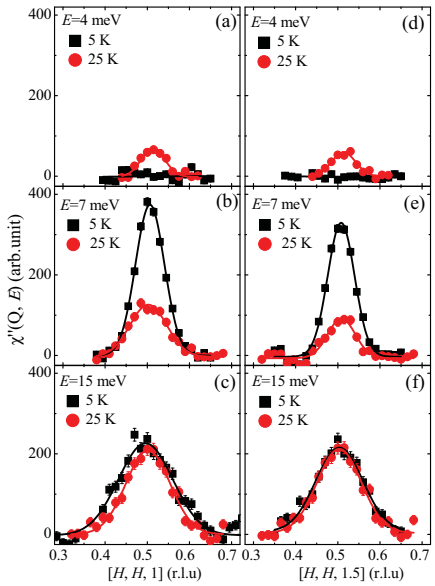

FIG. 3: **Constant-energy scans at different L values across T_c.** **Q** scans along the $[H, H, L = 1, 1.5]$ directions below and above $T_c = 18$ K at different energies: (a,d) in the gap (4 meV), (b,e) at the resonance (7 meV), and (c,f) above 2Δ (15 meV). The solid lines are fits to Gaussians. Data are from PUMA.

square of the Fe^{2+} magnetic form factor, thus confirming the two-dimensional and magnetic nature of the resonance.

In the optimally hole [11] and electron-doped $BaFe_2As_2$ [16, 17, 19], the resonances form longitudinally and transversely elongated ellipses, respectively. Since $NaFe_{0.935}Co_{0.045}As$ belongs to the electron-doped iron pnictide superconductor, we mapped out spin excitations in the $[H, K, 0]$ scattering plane on PUMA. Figures 4(c) and 4(d) show constant-energy scans at $E = 7$ meV along the transverse $[1/2 + H, 1/2 - H, 0]$ and longitudinal $[H, H, 0]$ directions, respectively, below and above T_c. Although there is no evidence for transverse incommensurate magnetic scattering as in the case of LiFeAs [30], the spin resonance in $NaFe_{0.935}Co_{0.045}As$ is considerably broader along the transverse direction than that of the longitudinal direction. Figure 4(g) shows the two-dimensional image of the resonance in the SC state, further confirming the results of Fig. 4(c) and 4(d).

Figure 4(e) and 4(f) summarizes the dispersions of the low-energy spin excitations along the longitudinal and transverse directions below and above T_c, respectively. In the normal state, spin excitations in $NaFe_{0.935}Co_{0.045}As$ are gapless, comparing with the $\sim$10 meV anisotropy gap in spin waves of the undoped NaFeAs [31]. On cooling to below T_c, the effect of superconductivity is to open a low-energy spin gap and concurrently form a neutron spin resonance. The dispersions of spin excitations are essentially unaffected by superconductivity, but change more rapidly along the transverse direction with increasing energy.

Discussion and Conclusions To compare with the experiment, we have performed RPA spin-susceptibility calculation in the SC state, using the five-orbital tight-binding model taken from Ref. [32]. The details of the calculation procedure can be found in Refs. [33, 34]. Results for the s^{+-} and s^{++} pairing symmetries are given in Fig. 5. For $s^{\pm}$-pairing, a spin-resonance appears due to the inelastic scattering of the Bogoliubov quasiparticles whose energy and wave vector can approximately be determined from $\omega_Q = |\Delta_{\mathbf{k}_F}| + |\Delta_{\mathbf{k}_F+\mathbf{Q}}|$ given that $\mathrm{sign}[\Delta_{\mathbf{k}}] \neq \mathrm{sign}[\Delta_{\mathbf{k}+\mathbf{Q}}]$, where $\Delta_{\mathbf{k}} = \Delta_0(\cos k_x + \cos k_y)$. There are two reasons for the resonance shift to $\omega < 2\Delta_0$: (1) Due to large area of electron pocket in these systems [35], the effective gap value on the Fermi momenta is reduced, i.e. $|\cos k_{xF} + \cos k_{yF}| < 1$. (2) The resonance energy shifts further to lower energy within RPA [33]. We take $\Delta_0 \approx 6$ meV [35–37] to obtain a resonance at 7 meV, in accord with experimental value. For the s^{++} pairing, due to the lack of sign-reversal, the spin-excitation inside the SC gap is completely eliminated. However, at $\omega > 2\Delta_0$, a hump like feature with intensity appears. The many-body RPA correction shifts the hump to a higher energy (for the same value of $U = 1.6$ meV, we obtain a weak feature around $\omega = 1.3(2\Delta)$), as shown in Fig. 5(b) and 5(c). With varying U as well as the intrinsic broadening, we find that the result is robust and the resonance peak in the $s^{\pm}$ is ubiquitously sharper than that for the s^{++}−case. Therefore, the neutron scattering results are consistent with $s^{\pm}$-pairing symmetry, eliminating s^{++}-pairing symmetry as a candidate for superconductivity.

Acknowledgements The single crystal growth efforts and neutron scattering work at UT are supported by

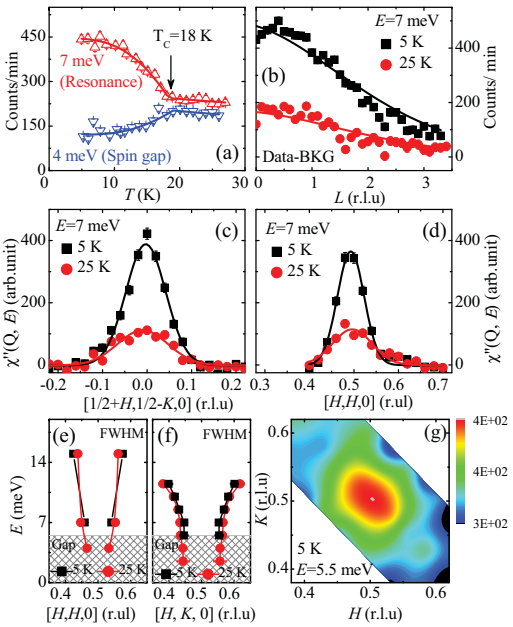

FIG. 4: **Temperature dependence of the resonance and spin gap.** (a) Temperature dependence of the scattering at $\mathbf{Q} = (0.5, 0.5, 1.5)$ at $E = 4$, and 7 meV. The solid lines show the order parameter fits by using $I = I_o + K(1-(T/T_c))^{\beta}$ yielding T_c 18.8 K for both. (b) Background subtracted constant energy scans with $E = 7$ meV along the $[0.5, 0.5, L]$ direction at 5 and 25 K. Background was taken at $\mathbf{Q} = (0.65, 0.65, L)$. The solid lines are the square of the Fe^{2+} form factor. (c) and (d) $\mathbf{Q}$-scans below and above T_c along the $[1/2 + H, 1/2 - H, 0]$ and $(H, H, 0)$ directions, respectively. (e) and (f) The dispersions of spin excitations below and above T_c along the $[H, H, 0]$ and $[H - \delta, K + \delta, 0]$ directions, respectively. The shaded area indicates the size of the spin gap in the SC state. (g) The in-plane wave vector profile of the $E = 5.5$ meV spin excitations in the SC state. Data are from PUMA.

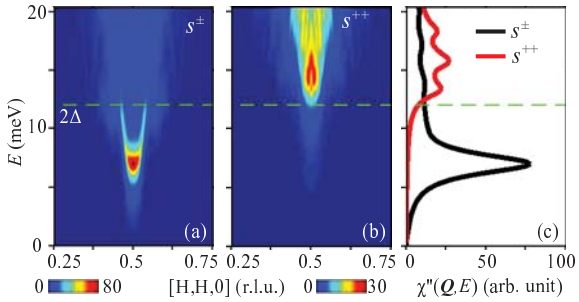

FIG. 5: **RPA calculated resonance for $s^{\pm}$ and s^{++} pairing symmetries.** (a) Computed spin-excitation spectrum for $s^{\pm}$ pairing channel. (b) Same but for s^{++} pairing symmetry. (c) $\chi''(\omega)$ at the AF wave vector $\mathbf{Q}$ for both these cases. The horizontal lines mark the $2\Delta_0$ line, below and above which the resonance occurs in the two cases, respectively. Both calculations are performed with fixed intrinsic broadening of 1 meV, SC gap of Δ_0=6 meV, and Coulomb interaction U=1.6 eV.

the US DOE, BES, through contract DE-FG02-05ER46202. Work at IOP is supported by MOST (973 Project: 2012CB82400). The work at JCNS and RWTH Aachen University was partially funded by the BMBF under contract No. 05K10PA3. Work at LANL was supported by the NNSA of the US DOE under contract DE-AC52-06NA25396.

* Electronic address: chenglin@utk.edu
† Electronic address: pdai@utk.edu

[1] Tsuei, C. C. & Kirtley, J. R., Pairing symmetry in cuprate superconductors. Rev. Mod. Phys. **72**, 969-1016 (2000).
[2] Kamihara, Y., Watanabe, T, Hirano, M. & Hosono, H. Iron-based layered superconductor La[$O_{1-x}F_x$]FeAs (x =0.05-0.12)

with $T_c = 26$ K. J. Am. Chem. Soc. **130**, 3296-3297 (2008).
[3] Rotter, M., Tegel, M., & Johrendt, D., Superconductivity at 38 K in the iron arsenide $(Ba_{1-x}K_x)Fe_2As_2$. Phys. Rev. Lett. **101**, 107006 (2008).
[4] Chu, C. W., *et al.*, The synthesis and characterization of LiFeAs and NaFeAs. Physica C **469**, 326-331 (2009).
[5] Mazin, I. I., Singh, D. J., Johannes, M. D., & Du, M. H., Unconventional superconductivity with a sign reversal in the order parameter of $LaFeAsO_{1-x}F_x$. Phys. Rev. Lett. **101**, 057003 (2008).
[6] Kuroki, K., Onari, S., Arita, R., Usui, H., Tanaka, Y., Kontani, H., and Aoki, H., Unconventional pairing originating from the disconnected Fermi surfaces of superconducting $LaFeAsO_{1-x}F_x$. Phys. Rev. Lett. **101**, 087004 (2008).
[7] Seo, K., Bernevig, B. A., and Hu, J. P., Pairing symmetry in a two-orbital exchange coupling model of oxypnictides. Phys. Rev. Lett. **101**, 206404 (2008).
[8] Korshunov, M. M., and Eremin, I., Theory of magnetic excitations in iron-based layered superconductors. Phys. Rev. B **78**, 140509(R) (2008).
[9] Maier, T. A., and Scalapino, D. J., Theory of neutron scattering as a probe of the superconducting gap in the iron pnictides. Phys. Rev. B **78**, 020514(R) (2008).
[10] Christianson, A. D. *et al.*, Unconventional superconductivity in $Ba_{0.6}K_{0.4}Fe_2As_2$ from inelastic neutron scattering. Nature **456**, 930-932 (2008).
[11] Zhang, C. L. *et al.*, Neutron Scattering Studies of spin excitations in hole-doped $Ba_{0.67}K_{0.33}Fe_2As_2$ superconductor. Scientific Reports **1**, 115 (2011).
[12] Castellan, J.-P. *et al.*, Effect of Fermi surface nesting on resonant spin excitations in $Ba_{1-x}K_xFe_2As_2$. Phys. Rev. Lett. **107**, 177003 (2011).
[13] Lumsden, M. D. *et al.,* Two-dimensional resonant magnetic excitation in $BaFe_{1.84}Co_{0.16}As_2$. Phys. Rev. Lett. **102**, 107005 (2009).
[14] Chi, S. *et al.,* Inelastic neutron-scattering measurements of a three-dimensional spin resonance in the FeAs-based $BaFe_{1.9}Ni_{0.1}As_2$ superconductor. Phys. Rev. Lett. **102**, 107006 (2009).
[15] Inosov, D. S. *et al.,* Normal-state spin dynamics and temperature-dependent spin resonance energy in an optimally doped iron arsenide superconductor. Nat. Phys. **6**, 178 (2010).
[16] Lester, C. *et al.* Dispersive spin fluctuations in the nearly optimally doped superconductor $Ba(Fe_{1-x}Co_x)_2As_2$ ($x = 0.065$). Phys. Rev. B **81**, 064505 (2010).
[17] Park, J. T. *et al.,* Symmetry of spin excitation spectra in tetragonal paramagnetic and superconducting phases of 122-ferropnictides. Phys. Rev. B **82**, 134503 (2010).
[18] Zhao, J. *et al.*, Neutron spin resonance as a probe of the superconducting energy gap of $BaFe_{1.9}Ni_{0.1}As_2$ superconductors. Phys. Rev. B **81**, 180505(R) (2010).
[19] Liu, M. S. *et al.*, Nature of magnetic excitations in superconducting $BaFe_{1.9}Ni_{0.1}As_2$. Nat. Phys. **8**, 376-381 (2012).
[20] Inosov, D. S. *et al.*, Crossover from weak to strong pairing in unconventional superconductors. Phys. Rev. B **83**, 214520 (2011).
[21] Onari, S., Kontani, H., and Sato, M. Structure of neutron-scattering peaks in both s++-wave and s-wave states of an iron pnictide superconductor. Phys. Rev. B **81**, 060504(R) (2010).
[22] Onari, S., Kontani, H., Neutron inelastic scattering peak by dissipationless mechanism in the s^{++}-wave state in iron-based superconductors. Phys. Rev. B **84**, 144518 (2011).
[23] Nagai, Y., & Kuroki, K., Determination of the pairing state in iron-based superconductors through neutron scattering. Phys. Rev. B **83**, 220516(R) (2011).
[24] Sato, M., Kobayashi, Y., Lee, S. C., Takahashi, H., Satomi, E., and Miura, Y., Studies on effects of impurity doping and NMR measurements of La 1111 and/or Nd 1111 Fe-pnictide superconductors. J. Phys. Soc. Jpn. **79**, 014710 (2010).
[25] Onari, S. and Kontani, H., Violation of Anderson's theorem for the sign-reversing s-wave state of iron-pnictide superconductors. Phys. Rev. Lett. **103**, 177001 (2009).
[26] Fernandes, R. M., *et al.*, Effects of nematic fluctuations on the elastic properties of iron arsenide superconductors. Phys. Rev. Lett. **105**, 157003 (2010).
[27] Li, S. L., Structural and magnetic phase transitions in $Na_{1-\delta}FeAs$. Phys. Rev. B **80**, 020504(R) (2009).
[28] Parker, D. R., *et al.*, Control of the competition between a magnetic phase and a superconducting phase in cobalt-doped and nickel-doped NaFeAs using electron count. Phys. Rev. Lett. **104**, 057007 (2010).
[29] A. F. Wang, X. G. Luo, Y. J. Yan, J. J. Ying, Z. J. Xiang, G. J. Ye, P. Cheng, Z. Y. Li, W. J. Hu and X. H. Chen, Phase diagram and calorimetric properties of $NaFe_{1-x}Co_xAs$. arXiv:1204.3522
[30] Qureshi, N. *et al.*, Inelastic neutron-scattering measurements of incommensurate magnetic excitations on superconducting LiFeAs single crystals. Phys. Rev. Lett. **108**, 117001 (2012).
[31] Park, J. T., *et al.*, Similar zone-center gaps in the low-energy spin-wave spectra of NaFeAs and $BaFe_2As_2$. arXiv:1204.0875.
[32] Graser, S. *et al.*, Near-degeneracy of several pairing channels in multiorbital models for the Fe-pnictides. New J. Phys. **11**, 025016 (2009).
[33] Das, T., and Balatsky, A. V., Two energy scales in the magnetic resonance spectrum of electron and hole doped pnictide superconductors. Phys. Rev. Lett. **106**, 157004 (2011).
[34] See supplementary materials for more information.
[35] Liu, Z. H.,*et al.*, Unconventional superconducting gap in $NaFe_{0.95}Co_{0.05}As$ observed by angle-resolved photoemission spectroscopy. Phys. Rev. B. **84**, 064519 (2011).
[36] Zhou, X. D. *et al.*, Evolution from unconventional spin density wave to superconductivity and a novel gap-like phase in $NaFe_{1-x}Co_xAs$. arXiv: 1204.4237.

[37] Yang, H. *et al.*, Unexpected weak spatial variation of local density of sates induced by individual Co impurity atoms in Na($Fe_{0.95}Co_{0.05}$)As as revealed by scanning tunneling spectroscopy. arXiv:1203.3123.